Acta Geodyn. Geomater.Vol.1, No.2 (134), 165-185, 2004

SURFACE WAVES DISPERSION CURVES OF EURASIAN EARTHQUAKES: THE SVAL PROGRAM

Petr KOLÍNSKÝ

Institute of Rock Structure and Mechanics, Academy of Sciences of the Czech Republic, Prague, V Holešovičkách 41, 182 09 Praha 8, Czech Republic
Corresponding author's e-mail: kolinsky@irsm.cas.cz

(*Received* August 2003, *accepted* December 2003)

ABSTRACT
A summary of seismic surface waves and time-frequency analysis theory is presented here. The main goal is to introduce the multiple-filter technique, which is to be used for processing of records. The SVAL program has been built and tested. The SVAL computes the spectrogram of a given signal, a filtered spectrogram, a filtered seismogram and group velocity dispersion curves of Rayleigh and Love fundamental modes. Filtered seismograms reveal also other wavegroups contained in a record of each component. The dispersion of overtones and Rayleigh waves at a transverse component and Love waves at vertical and radial component is also studied. The function of the program is demonstrated on Asian earthquakes recorded at the Praha seismic station.

KEYWORDS: surface waves, dispersion, group velocity, time-frequency analysis, multiple-filter technique

1. INTRODUCTION

Time-frequency analysis techniques are used to estimate the group velocity of seismic surface waves. Surface waves come up as a result of interference of body waves. The waves of different period propagate with different velocities; this phenomenon is called dispersion. As the surface wave velocities depend only on the structure and not on the focal mechanism, it allows determination of an average structure of the Earth crust between the epicenter and a seismic station.

Rayleigh waves are supposed to be found at the vertical and at the radial component of a recorded seismogram and Love waves at the transverse component. In fact, there is no clean group of a fundamental mode of these two types of waves to be seen on a real seismogram. In case of near earthquakes body waves are also recorded over the long periods of surface waves. Even if the difference between the arrival times of the body and surface waves is big enough to resolve the groups of waves in time domain, there can be overtones of both types of surface waves. After the main group of Rayleigh and Love waves, there is often a surface wave coda. We can also see the modes at the "wrong" component and we can observe the detached parts of the same group of waves. These phenomena are caused by lateral heterogeneity of the Earth crust where the surface waves can propagate differently from the geometrical great circle path and where the same waves can propagate along different paths respectively. The latter phenomenon is called multipathing. Due to the heterogeneity, we can find Rayleigh waves at the transverse component and Love waves at the radial component. Due to anisotropy, Love waves can be recorded also at the vertical component.

There are differences in the surface wave propagation along continental and oceanic paths because of the layer of water where shear waves cannot propagate and also because of a thinner oceanic Earth crust in which the waves have higher velocities than in a thicker continental crust. Oceanic crust is more laterally homogeneous than the continental one. The period range where waves of a bit different periods in the same time arrive is called Airy phase. The broad spectrum is summed up here so that the amplitudes are higher.

The problem is not only to determine the dispersion of the fundamental mode, but also to find out this mode among the recorded wavegroups and to reduce the non-required body waves, overtones, multipathed parts of waves, coda and Rayleigh and Love waves at "wrong" components in the seismogram.

In this paper, we present a method for the estimation of surface waves group velocities. We also show how to create a filtered seismogram and how to use its comparison with the raw one for better

determination of each group of waves. Moreover, we try to estimate the dispersion curves for previously non-required parts of the seismogram and by filtering and comparing we demonstrate further their presence in the recorded waveform. Four examples of surface waves analysis of Asian earthquakes recorded at the Praha seismic station are presented.

2. TECHNIQUES OF TIME-FREQUENCY ANALYSIS

The aim of time-frequency analysis is to study the properties of signal both in time and frequency domain. For wavegroups of different arrival times the time domain is good enough to distinguish each of the groups from another. In case of signal composed of a few harmonic components, we can distinguish them using a frequency domain. When studying surface waves, we need both these attitudes at the same time because of the dispersion. The frequency content of signal varies with time.

Traditional time-frequency technique was "the peak and trough technique". This technique is not used very often now, because signals are recorded and processed digitally by computers. At present, we can speak about two basic types of methods (Kocaoglu and Long, 1993): the decomposition methods based on Fourier or wavelet transformations (and others) and the methods using the time-frequency distributions. We will deal with a method based on the Fourier transform in this paper (Čermák, 1990; Sekereš, 1983). In the next paragraphs we will also use terms of linear filtering theory.

The time-frequency representation can be defined in form of an integral $S(\omega,t)$ in time domain as

$$S(\omega,t)=\int_{-\infty}^{+\infty} f(\tau)k(\omega,t-\tau)d\tau, \tag{1}$$

where t is time and ω is angular frequency. Symbol $f(t)$ represents signal and $k(\omega,t)$ is a complex kernel. That is why the integral $S(\omega,t)$ is also complex. We integrate by τ variable. For each fixed angular frequency ω this definition can be understood as a convolution of signal $f(t)$ with the kernel $k(t)$. The kernel $k(\omega,t)$ is often called an impulse response of the filter.

If we choose the kernel in form $k(\omega,t)=w(t)\cdot e^{i\omega t}$ we obtain the integral by formula

$$S(\omega,t)=\int_{-\infty}^{+\infty} f(\tau)w(t-\tau)e^{i\omega(t-\tau)}d\tau. \tag{2}$$

The signal $f(t)$ is weighted with the function $w(t)$, which slides along the signal and selects only a small part of it at each time t. Then we make a Fourier transform of this selected part of signal. This method of computing a time-frequency representation is called "the moving-window technique".

We can also define the same integral $S(\omega,t)$ in the frequency domain as

$$S(\omega,t)=\frac{1}{2\pi}\int_{-\infty}^{+\infty} F(\Omega)K(\omega,\Omega)e^{i\Omega t}d\Omega\,. \tag{3}$$

$F(\Omega)$ is a spectrum of the signal $f(t)$ and $K(\omega,\Omega)$ is a spectrum of the impulse response $k(\omega,t)$. We can understand $K(\omega,\Omega)$ as a transfer function of the filter. If we choose the same kernel $k(\omega,t)=w(t)\cdot e^{i\omega t}$ as in the latter case, we obtain transfer function as

$$K(\omega,\Omega)=W(\Omega-\omega) \tag{4}$$

and the integral $S(\omega,t)$ can be written as

$$S(\omega,t)=\frac{1}{2\pi}\int_{-\infty}^{+\infty} F(\Omega)W(\Omega-\omega)e^{i\Omega t}d\Omega. \tag{5}$$

The signal spectrum $F(\Omega)$ is weighted with the filtering function $W(\Omega-\omega)$ and then the result is transformed back to the time domain. The weighting function $W(\Omega-\omega)$ is centered to the frequency ω. For each frequency ω it selects only the part of the spectrum $F(\Omega)$ near this frequency. This method is called "the multiple-filter technique" or "the multi-channel filtering". An example of such filtering is shown in Fig. 1.

We define the spectrogram $P(\omega,t)$ as the squared modulus of complex integral $S(\omega,t)$:

$$P(\omega,t)=\left|S(\omega,t)\right|^2. \tag{6}$$

The time-frequency representation $P(\omega,t)$ presents a distribution of energy of signal both in time and frequency domain. In this paper, we concentrate on the multiple-filter technique of computing $P(\omega,t)$. The results of moving-window and multiple-filter techniques are equivalent theoretically, but there can be some numerical differences. Multiple-filter technique is easier to adjust the parameters of filtering via a transfer function according to the properties of a spectrum of a given signal and according to the wanted characteristics of the computed spectrogram.

The uncertainty principle belongs to the main properties of Fourier transform. The localization of energy in the spectrogram is influenced by the length of time window $w(t)$ in case of the moving-window technique and by the broadness of the filter $W(\Omega)$ in case of the multiple-filter technique. We cannot achieve arbitrary resolution in both domains. If we use shorter time window to improve localization in time domain, we obtain broader local spectrum in

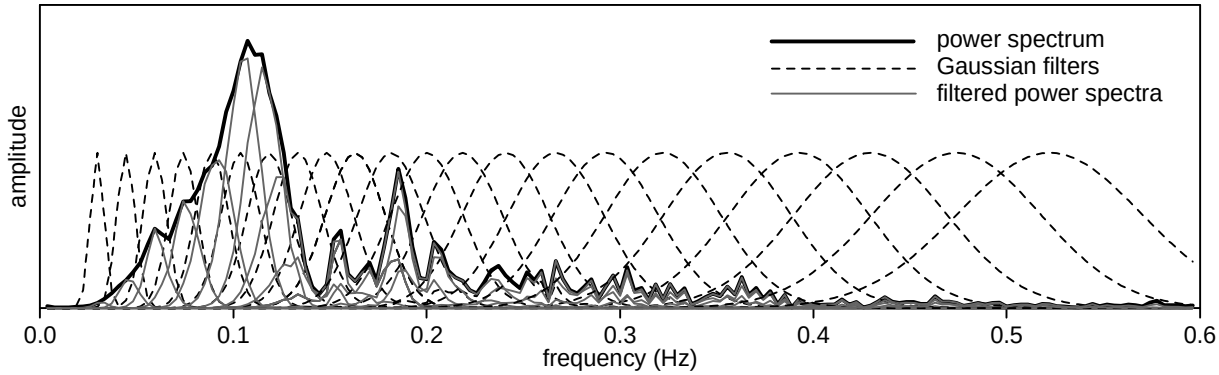

Fig. 1 Filtering by using constant relative resolution, Gaussian, frequency domain filters as an instrument of multiple-filter technique. Amplitude power spectrum of real earthquake record is drawn (bold solid line). Gaussian filters (dashed lines), used for weighting the spectrum, are shown. The results of filtering using these filters are also drawn (gray lines). The frequency step is bigger and the filters are broader towards the high frequencies. The amplitudes of spectrum and Gaussian filters are mutually not in the scale. This example presents a spectrum of the transverse component record of the earthquake in Turkey, see Tab. 1. The other examples of the SVAL program function presented in this paper are also based on this record as mentioned in the corresponding figure captions.

frequency domain. When using narrow filter in frequencies, we obtain worse resolution in time.

The uncertainty principle is expressed as

$$\Delta t \Delta \omega \geq \frac{1}{2} \tag{7}$$

where Δt means the length of impulse in time domain and $\Delta\omega$ is the broadness of response in the frequency domain. If we use the Gaussian filter as a transfer function in the shape of

$$K(\Omega) = Ae^{-\alpha\Omega^2}, \tag{8}$$

where A is an arbitrary constant and α is a positive parameter, we achieve the equality in expression (7) and therefore the best resolution both in frequency and time domain. The impulse response (a Fourier transform of the transfer function) is also Gaussian function.

According to (4) we can use the filtering function W for example as

$$W(\Omega - \omega) = e^{-\alpha(\Omega-\omega)^2}. \tag{9}$$

The process of using such weighting function is called "the constant resolution filtering". The filter bandwidth controlled by $(\Omega - \omega)$ is constant for all the central frequencies ω. The drawback of this filtering is that we cannot approach low frequencies ω. To get the well defined spectrogram, we need to keep $\omega > (\Omega - \omega)$. This condition is not kept for the low central frequencies ω and the filter is not narrowband. For $\omega \to 0$ the weighting function W selects too broad part of a spectrum to localize the energy well.

To improve this, we can use "the constant relative resolution filtering" (Dziewonski et al., 1969). The filtering function W is expressed as

$$W(\Omega - \omega) = e^{-\alpha\frac{(\Omega-\omega)^2}{\omega^2}}. \tag{10}$$

For the lower central frequencies ω the absolute value of filter bandwidth is narrower but the relative bandwidth controlled by $(\Omega - \omega)/\omega$ remains constant. We do not use the whole theoretical range of $\Omega \in (-\infty;+\infty)$ but only narrower range estimated according to the number of record samples. For $\omega \to 0$ the bandwidth of filters decreases to keep the resolution of energy constant in frequency domain. This type of filters is shown in Fig. 1. We will deal with such a filtering in this paper.

We have not discussed the parameter α yet. It is possible to change the width of the filter by increasing or decreasing this parameter. If α is constant for all the used central frequencies, we talk about "the homogeneous filtering". If α varies with the central frequency, it is called "the optimal filtering". By increasing the parameter α towards low frequencies, we intensify the effect of the constant relative resolution filtering and by decreasing α we lower this effect.

The SVAL program, which was built to compute spectrograms and other quantities concerning the dispersion of surface waves, uses the constant relative

resolution optimal Gaussian filtering as a tool of multiple-filter technique.

Consider a particular component of an earthquake record. First of all the complex Fourier spectrum of this record is computed. After that this spectrum is filtered. It means that both the real and the imaginary parts of the spectrum are multiplied by the set of weighting functions $W(\Omega-\omega)$ for selected (see next paragraphs) central frequencies ω (or periods T). The filtering is applied on the positive frequencies of the spectrum; the negative ones are not used in further processing. These filtered spectra are transformed back to the time domain. Using only the positive frequencies is the way to obtain an analytic signal $f_a(t)$, corresponding to the original record $f(t)$ and its spectrum $F(\Omega)$, as it is expressed by

$$f_a(t) = \int_0^\infty F(\Omega) e^{i\Omega t} d\Omega, \tag{11}$$

see Červený (2001). The real part of analytical signal equals the original real signal and the imaginary part presents the Hilbert transform of the original signal (a signal with phase shift of $\pi/2$). Modulus of an analytical signal given as

$$|f_a(t)| = \sqrt{[\mathrm{Re}\, f_a(t)]^2 + [\mathrm{Im}\, f_a(t)]^2}, \tag{12}$$

presents an envelope of original record.

We obtain a set of nearly monochromatic complex signals of selected frequencies $S(\omega_{const}, t)$. The real parts of such signals are shown in Fig. 2. A squared modulus of complex $S(\omega_{const}, t)$ amplitude is computed according to the expression

$$P(\omega_{const}, t) = [\mathrm{Re}(S(\omega_{const}, t))]^2 + [\mathrm{Im}(S(\omega_{const}, t))]^2, \tag{13}$$

We obtain an envelope of the nearly monochromatic signal, also drawn in Fig. 2. This envelope represents a distribution of energy carried by a wave of a given period. The time frequency representation $P(\omega, t)$ is created by drawing such envelopes side by side according to their central period. In fact, the signals $S(\omega_{const}, t)$ are not exactly monochromatic. After the program finds the time t_0 (see next paragraphs) when the maximum of energy arrives, the instantaneous frequency of this moment is computed according to the expression (see Červený, 2001)

$$f_{inst}(t_0) \cong \frac{1}{2\pi} \left. \frac{d\Phi(t)}{dt} \right|_{t=t_0}, \tag{14}$$

where $\Phi(t)$ is the phase of an analytical signal $f_a(t)$ given as

$$\Phi(t) = -\arctan\left(\frac{\mathrm{Im}(f_a(t))}{\mathrm{Re}(f_a(t))} \right). \tag{15}$$

These instantaneous frequencies $f_{inst}(t_0)$ or the instantaneous periods $T_{inst}(t_0) = 1/f_{inst}(t_0)$ are used for drawing the envelopes in appropriate places to create the spectrogram instead of the original central periods. Obtained amplitudes of spectrogram $P(\omega, t)$ are normalized according to 100 dB scale. We will discuss the details of the computing process in the next paragraphs.

3. ESTIMATION OF SURFACE WAVES GROUP VELOCITY

By the term "dispersion curve", we mean the dependence of group velocity U on the period T (or frequency ω or f) of the wavegroup. The Fourier transform of short-time window should display an amplitude maximum at the prevailing frequency, which occurs in this window. Using the multiple-filter technique, the inverse Fourier transform of each spectrum filtered on given period T should display an amplitude maximum at the time t_g when the energy of a wave of the period T arrives.

The dispersive group velocity $U(T)$ can be expressed as

$$U(T) = \frac{\Delta}{t_g(T)}, \tag{16}$$

where Δ is an epicentral distance. And therefore if we find the arrival time of the wavegroup for a given period, we obtain one point of the dispersion curve for the record of a known epicentral distance. Otherwise if we find local maxima of a spectrogram for each filter centered on given periods, we can draw the dispersion curve. For imaging the spectrogram we do not use the time-frequency diagram but the group velocity-period diagram. Instead of $P(\omega, t)$ we draw $P(U, T)$; that can be expressed by $P(\Delta/t, 2\pi/\omega)$, when using original variables, because the period $T = 2\pi/\omega$.

The SVAL program works exactly this way. It takes each envelope of the nearly monochromatic signal created by filtering of the Fourier spectrum of the raw signal and finds the time t_g, which belongs to the amplitude maximum of this envelope. Time t_g is connected with the group velocity according to the expression (16).

In Fig. 6 we see a main dispersion ridge at the spectrogram computed for a transverse component of the Turkish earthquake (see Tab. 1) recorded at the Praha seismic station. This ridge represents the dispersion curve that we want to estimate. But there

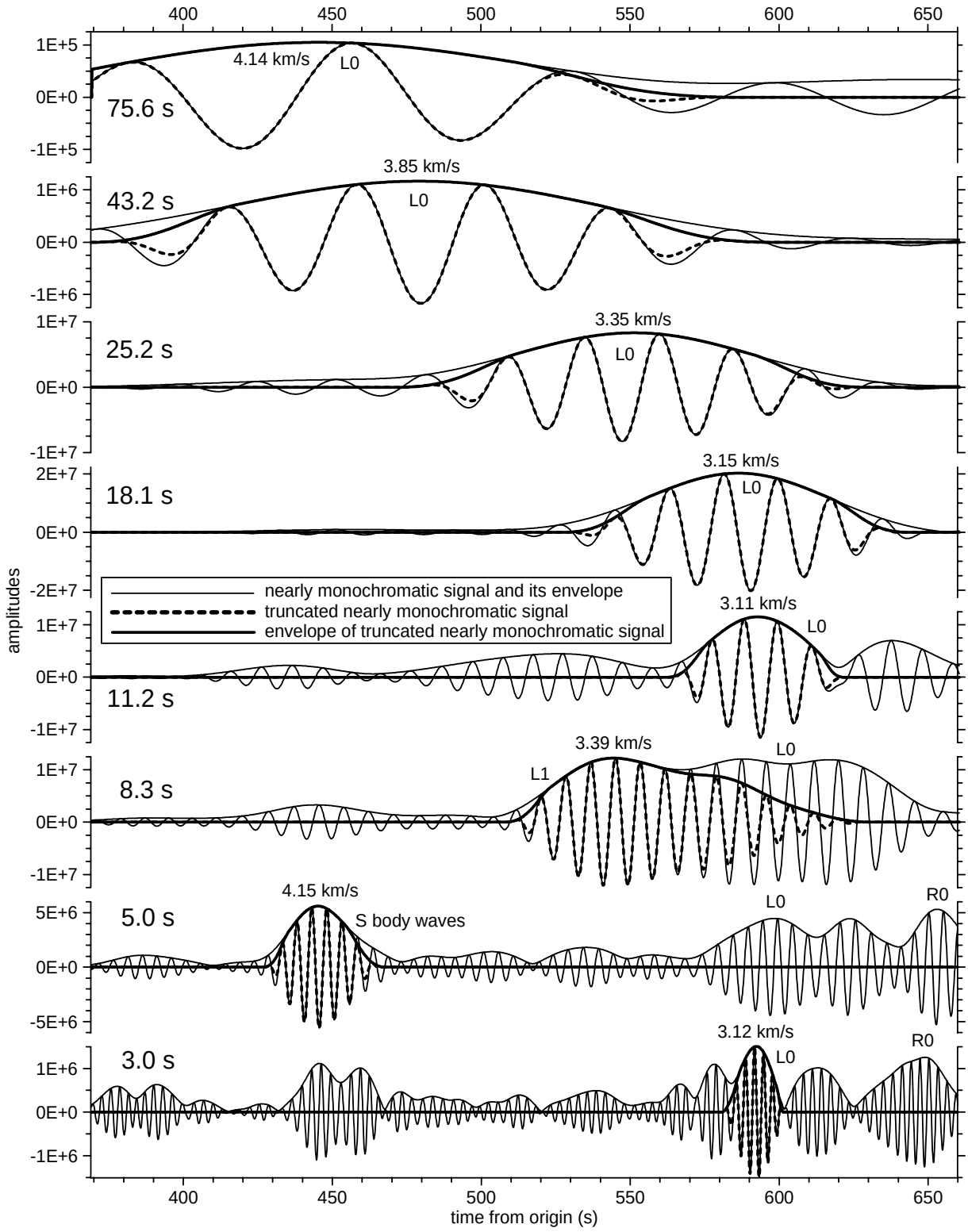

Fig. 2 The thin solid lines represent the real parts of nearly monochromatic complex signals and their envelopes. Bold solid lines represent the truncated and smoothed envelopes and bold dashed lines the truncated and smoothed real parts of nearly monochromatic complex signals. Eight filters were selected for this figure from more than hundred filters used during the processing of the transverse component of the Turkish earthquake record (see Tab. 1). Compare the filtered wavegroups at each period with the upright rectangle in Fig. 6 where the filtered spectrogram of the same component is shown. At period 5.0 s the S wave was filtered out of the signal. At period 8.3 s the first higher mode of Love wave was found. For longer periods the wanted fundamental mode was filtered out. At period 3.0 s again the fundamental mode was found (not showed in Fig. 6). For periods 3.0, 5.0 and 8.3 s the filtered, nearly monochromatic signal, contains a few wavegroups and it is not always clear what mode they belong to. Group velocities of selected wavegroups are marked. Notice that the amplitudes of filtered signals are not in the scale.

Table 1 The table shows parameters concerning the four events presented in this paper. The back azimuth assigns the direction from the Praha seismic station to the epicenter.

Country	Date (dd/mm/yy)	Origin time (UTC) hh : mm : ss.ss	Latitude (N)	Longitude (E)	Depth (km)	Magnitude	Epic. distance (km)	Back azimut (h)
Turkey	03 / 02 / 02	07 : 11 : 28.41	38.57	31.27	5	6.5 (M_w)	1846	127.4^0
Tibet	28 / 03 / 99	19 : 05 : 11.03	30.51	79.40	15	6.6 (M_s)	5731	86.5^0
Taiwan	31 / 03 / 02	06 : 52 : 50.49	24.28	122.18	32	7.4 (M_s)	9149	61.1^0
Kamtchatka	08 / 03 / 99	12 : 25 : 48.99	52.06	159.52	56	7.0 (M_w)	8217	21.5^0

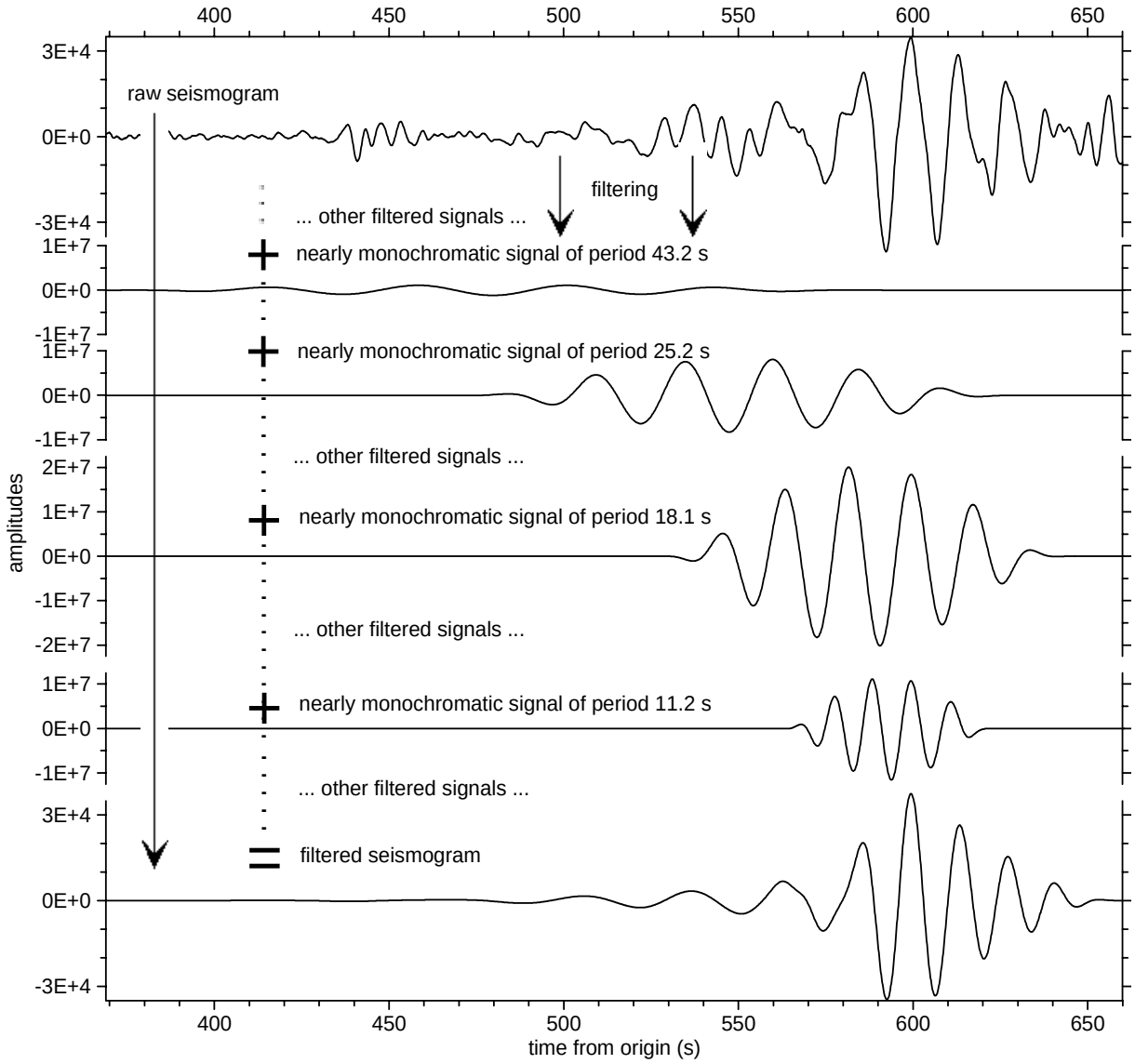

Fig. 3 Four truncated and smoothed real parts of nearly monochromatic signals presented in Fig. 2 are used to show, how the filtered seismogram is created. In Fig. 2, they are drawn by bold dashed lines. In fact, the filters of the period range from 11.0 to 105.0 s were used for summing up of this filtered seismogram. The original raw seismogram is also drawn. The amplitude scales of all four nearly monochromatic signals are the same. For comparing filtered and raw seismograms see Fig. 7.

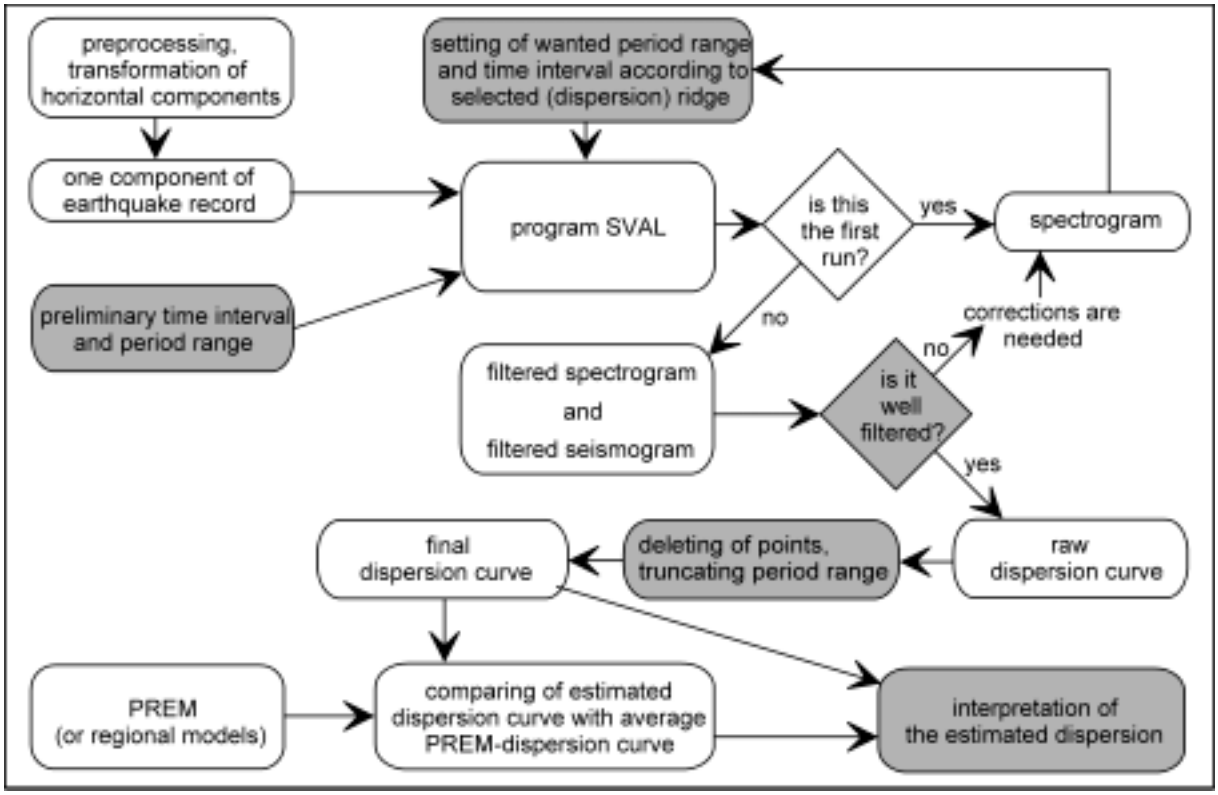

Fig. 4 The diagram shows the process of computing the dispersion curves using the SVAL program. Grey-filled frames represent the steps where human decision has to be made.

are also several other ridges or peaks at the spectrogram. If their amplitudes are lower than the amplitudes of the main dispersion ridge, the process can work as it was mentioned before. But for example coda can contain higher amplitudes and therefore the selected maxima for each nearly monochromatic signal will jump from the main ridge to the coda ridge. To draw the dispersion curve of a fundamental mode, we need to separate it from the rest of the wavefield.

First of all we have to determine what parts of the spectrogram really belong to the main dispersion ridge. By truncating the part of the spectrogram containing coda, we can help the program to find the maxima on the required ridge. In case of the mentioned earthquake, we truncate the spectrogram at the velocity of 2.8 km/s. We also do not need to look for the dispersion in the front part of a record because a surface wave fundamental mode cannot propagate with such high velocities. That is why we truncate also the velocities higher than 5.0 km/s. There is no ridge visible over the period 110 s. We can see a few smaller ridges of the same amplitudes in a period shorter than 5.0 s. We are not sure, which of them belongs to the main dispersion ridge and estimated dispersion curve will probably again jump from one peak to another. So we kept only a square cut off of the spectrogram for the computation of fundamental L_0 mode dispersion as marked in Fig. 6.

The work of the SVAL program branches here. To create the filtered seismogram containing only the waves of selected mode we need to select the whole ridge as it is viewed on the right side of Fig. 6. According to the estimated dispersion curve the program selects a broader part of the spectrogram. It keeps the maximum of each nearly monochromatic signal envelope and finds the two nearest inflection points. One of these points is before the envelope maximum and the other behind it. By a linear extrapolation according to the derivation of the inflection points the two zero points are found. The signal envelope between the two inflection points is kept, both parts of signal between the inflection and zero points are smoothed by the cosine window to the zero amplitudes and the rest is truncated. This process is applied not only on the signal envelopes but also on the nearly monochromatic complex signals. The same time values of inflection and zero points found at the signal envelope are used for a corresponding signal. Examples of this selection are shown in Fig. 2.

By completing such truncated and smoothed normalized envelopes the program creates a filtered

spectrogram. According to this, we can check our assumption concerning the selection of the main dispersion ridge from the original spectrogram. In Fig. 6 there are three wrongly filtered parts of the L_0-filtered spectrogram: between periods 8.0 and 9.0 s, there is a peak, which belongs to overtone L_1 and the filtered spectrogram contains a trace of it. Between periods 5.3 and 8.0 s the R_0 wavegroup trace is present and for the periods shorter than 5.3 s the filtering selected the ridge of body S-wave. Such parts of the filtered spectrogram show that the corresponding parts of the dispersion curve should be removed.

The program sums up all the truncated and smoothed real parts of nearly monochromatic signals and creates the filtered seismogram by normalizing amplitudes of the result of a summing according to the raw seismogram. Process of the summing of the filtered seismogram is shown in Fig. 3. When comparing it with the raw one, we can see what part of the original signal belongs to a selected wavegroup. For example the trace of L_1 mode contained at filtered spectrogram of L_0 mode made also the inappropriate signal in L_0-filtered seismogram. In Fig. 7, this filtered seismogram only for periods longer than 11.0 s is shown.

The other output branch of the SVAL program creates the dispersion curve. We can compare the result with dispersion curves computed for the PREM model (Dziewonski and Anderson, 1981). It is another opportunity to check the filtration of spectrogram. As we can see on Fig. 6, the filtered spectrogram for fundamental mode of Rayleigh waves R_0 can be considered to belong to a continuously dispersed wavefield but this ridge is built of two different wavegroups. For periods longer than 22 s the filtered ridge does not belong to the Rayleigh waves; it is a coda coming after the Love wave fundamental mode. The group velocities of Rayleigh waves for this period range should be the same as for Love waves and therefore they are hidden in the main dispersion ridge, if they are actually present. Such a conclusion can be supported by comparing spectrogram of transverse component with both the vertical and the radial component spectrograms. In case of this event, strong group of Rayleigh waves is present at these components as we can see in Fig. 8.

As we selected the main dispersion ridge of fundamental mode, we can continue by selecting other smaller ridges. In Fig. 6 filtration for R_0 mode of Rayleigh waves is shown, as mentioned above, and also for the first higher mode of Love waves L_1. It is well visible in Fig. 7 that an original seismogram contains two different components: in the same time interval the periods about 30 – 50 s of fundamental mode and periods about 6 – 11 s of the first higher mode are present here. The last cut rectangle in Fig. 6 shows the S-wavegroup. There is no dispersion of velocities but the filtered seismogram, drawn in Fig. 7, clearly shows this group in context of other features of original signal. The dispersion curves, estimated for three dispersed wavegroups presented in Fig. 6, are drawn in Fig. 8.

The process of estimation, also shown in Fig. 4, is explained in the following paragraph: First we see the spectrogram drawn as group velocity-period diagram computed by the program. Then we have to select the range of periods and group velocities (time) for computing the dispersion of only one of the modes. Now we have the filtered spectrogram to check the previous selection. We can also compare the filtered seismogram with the raw one to check the same thing by different attitude – if the filtration of the spectrogram had really selected only one of the wavegroups. If it seems to keep a continuous ridge, we can draw the dispersion curve. The wrongly filtered points, which do not belong to a wanted dispersion ridge, can be deleted. In the next step, we can compare the estimated curves with some of the other results mentioned in literature (PREM).

Only by analyzing one of the ridges of one component of the earthquake record, we can usually select and recognize all the other wavegroups. In case of earthquakes of epicentral distances such as thousands of kilometers, the modes of surface waves (and also body waves) are well visible and separated in time domain. Their group velocities are usually close enough to the average velocities of PREM which enables to estimate the wavegroup type. In each of the steps described above, we have to check the selecting the very part of spectrogram we have done and if there is a suspicion of a wrong filtering, we have to change the range of periods and time interval on the input of the SVAL program.

There are three steps of the process coupled together: computing of a filtered spectrogram, filtered seismogram and dispersion curve. But to demonstrate each of the features, we may need different input parameters of computing by the SVAL program. In case of the fundamental mode L_0 we have selected the range of periods and time interval which enables us to compute the filtered spectrogram. Even though there are some disturbances it is clearly visible, which parts of it belong to the main dispersion ridge and which parts do not. For drawing of filtered seismogram we have used only the periods longer than 11.0 s. It enables us to show the difference between two Love wave modes. It is not necessary to deal with the shorter periods presented by weak amplitudes in the end of L_0 mode but this narrower range has eliminated the disturbing trace of L_1 mode contained at the filtered spectrogram. In fact we estimated the dispersion curve for the broad range of periods from 9 to 105 s, see Fig. 8.

In case of the vertical and the radial components of the Turkish event, shown in Fig. 8, we estimated discontinuous dispersion curves for R_1 mode of Rayleigh waves. Several points in group velocity-period diagram had to be deleted. On the other hand the filtered seismograms clearly show the R_1 mode wavegroup at both components.

In Fig. 7 the filtered seismogram of R_0 mode for the whole period range of R_0-filtered spectrogram in Fig. 6 is shown. As we mentioned before, this interpretation probably is not correct. In Fig. 8 we can see the R_0-filtered seismogram drawn only for shorter periods. In comparison with the two other components, we can see, that the short periods probably also does not belong to this mode because they are not present at these components, despite the fact that the velocities of the wavegroups at all the three components are the same. Thus the dispersion of R_0 mode has been estimated only for the interval 4 – 22 s at the transverse component of this event.

4. DETAILS CONCERNING THE COMPUTATIONAL PROCESS THE SVAL PROGRAM

The source text is written in Fortran 90 standard programming language. It is based on former work of Sekereš (1983) and Čermák (1990), but the source text is completely new. The program consists of the main program and several subroutines. We used up to 2^{14} samples in the computational process while studying the records of Asian earthquakes. There are comments explaining all the steps of computing in the source text.

PARAMETER INPUT FILE

The basic procedures of computing are controlled by input text file. It contains 9 rows with the following parameters: epicentral distance of the earthquake in kilometers, time interval between the origin time and the beginning of the record, the sampling frequency of the record, the maximal and the minimal central period of filtration, ordinal number of the sample to start reading record input file, number of samples to be used for computing spectrogram, maximal number of filters to be used and length of cosine window for smoothing the truncated ends of a raw record.

SMOOTHING WINDOW

Because the record used for computing is truncated at both sides and such a steep step in amplitudes would present an artificial high-frequency spectrum, the amplitudes are smoothed. The number of samples set in parameter input file is multiplied by the cosine function. This smoothing is also used for the truncated parts of nearly monochromatic signals and their envelopes during the filtration of spectrogram.

CENTRAL FILTERING PERIODS

The central periods between the minimal $T_{\min}$ and the maximal $T_{\max}$ periods are estimated. Each next T_{j+1} central period is derived from the given T_j as

$$T_{j+1} = \gamma \cdot T_j . \tag{17}$$

The multiplicative step γ is computed according to the number of filters N_{filt} to obtain

$$T_{\max} = \gamma^{N_{filt}-1} \cdot T_{\min} . \tag{18}$$

It means that the absolute value of the step between longer periods is greater than between the shorter ones, as seen in Fig. 1. The spectrogram is less complicated towards longer periods and for presentation, we use logarithmic scale which effectively suppresses this geometric step. The corresponding central frequencies are given as integers because they present an ordinal number of central sample. The equidistant step of central frequencies lower than 0.1 Hz (see also Fig. 1) is due to the sampling frequency in time domain (10 Hz), which produces limited sampling frequency in frequency domain. Towards low frequencies, the constant geometrical period step results in a smaller frequency step, than the sampled one, and some of the previously computed central frequencies are not used for filtering.

FOURIER TRANSFORM

Program uses Fast Fourier Transform. The explanation can be found in Press et al. (1992).

OUTPUT FILES

The SVAL program produces eight output files: a file containing three columns representing time, frequency and normalized amplitude which makes it possible to draw spectrogram, a file containing three columns representing periods, group velocity and normalized amplitude which enables to draw spectrogram in group velocity-period representation, a file containing the same type of data including filtered normalized amplitudes for imaging filtered spectrogram, files containing periods and group velocity for drawing dispersion curve with and without the time correction of the seismograph and a file of filtered seismogram. Two files, containing information about important steps of computing and about the central and estimated periods, are also produced. During adjusting of the filtering process it is recommended to keep the files because of better imaging of different surface waves analysis phenomena mentioned above.

IMAGING THE SPECTROGRAMS

Spectrograms are shown as rectangles. Their resolution is in order of tens or low hundreds in a scale of periods (number of used filters) and in order of hundreds and thousands in a scale of group velocities (number of record samples). If we used this resolution for imaging the spectrograms, there would be many small ridges belonging to each peak of the signal envelope on higher frequencies (see Fig. 2 – the nearly monochromatic signals filtered with the central periods 3.0 and 5.0 s) around the main dispersion ridge and overtones and it would not be possible to see the main properties of the signal in such an accessible way. For drawing the spectrograms, using colour scale, the real surface obtained by the multiple-filter technique was smoothed by "the nearest neighbor method". It is only a matter of graphical depiction and the process of looking for the local maxima for drawing the dispersion curves is not affected by this.

5. PARAMETERS ADJUSTING THE ESTIMATION OF DISPERSION CURVE PERIOD RANGE

This parameter can be set arbitrary, but only a specified range has physical meaning. In case of surface waves of distant earthquakes we do not study the periods shorter than 2 s and so there is no question of Nyquist frequency in case of sampling rate 10 Hz. The length of the longest period, which can be found, depends on the length of studied part of the record. The program checks whether the maximal period that should be estimated is not longer than half of the length of the selected record interval. It is possible to look for even longer periods but we cannot estimate the envelope of such periods well and therefore the maximum of energy is less accurately resolved. Despite using the long-period seismograph, there is often a constant plateau at the spectrograms in the range of periods over 50 s and the maximum of amplitudes has no meaning. Only the strongest events records contain well recorded periods over this range.

TIME INTERVAL

As mentioned above, this parameter is coupled with the period range. The time interval is the most important value to be changed for the selection of a dispersion ridge. But to select the given dispersion ridge, we have to reduce the time interval and therefore we obtain a less accurate group velocity for longer periods. In fact, the estimation of dispersion, belonging to the given ridge, is more critical in shorter periods. The overtones, coda and body waves have shorter periods than the fundamental mode of surface waves. To estimate group velocities of long periods and to obtain continuous dispersion curve, we had to choose longer time interval and increase the minimal period of multi-channel filtering. It means that by the SVAL program, it is not always possible to estimate the dispersion in a broad range of periods at the same time.

LENGTH OF SMOOTHING COSINE WINDOW

It is not a critical parameter. By using long window at the ends of truncated parts of record, we clean the short period part of spectrum, but it can seriously damage the amplitudes and period value estimation of weak long periods if the length of a window is of a value about half of the wavelength and the time interval is too short to contain more than two periods in the same moment. The used value of smoothing cosine window is 10 s. The length of the window used for smoothing the edges of the truncated nearly monochromatic signals and their envelopes is set by the program itself, as mentioned above.

COEFFICIENT α

This is the most important parameter to be set for multiple-filter technique process. As mentioned above, we control the relative width of the filter by changing this parameter. In case of constant relative resolution filtering, the absolute value of bandwidth is determined by the central frequency ω. For the lower central frequencies the bandwidth is narrower. Coefficient α appears in a numerator of the exponent ratio in the expression for filtering function (10) so by setting lower α, we obtain a broader filter. Due to the uncertainty principle, we cannot set α very high. It would make narrow filters, which would cause long unreal time signal and the resolution of the spectrogram would decrease. However, by setting α very low we make a very broad filter that will cause real signal in the time domain but this signal would be completed by lots of frequencies. It also decreases the resolution of the spectrogram. There is an optimal α which will keep the resolution of the spectrogram at the best level. On the other hand, the optimal value may change with the central frequencies. In this paper we shall use an optimal filtering.

Fig. 5 shows spectrogram of the same record using eight values of coefficient α constant for the whole period range (homogeneous filtering). It is clearly visible that for the low α the spectrogram is blurred in the direction of period (frequency) axis for lower periods but longer periods are better visible. In case of high α the spectrogram is blurred in the direction of the group velocity (time) axis for longer periods, but it is well estimated for the shorter ones. In the first case, we cannot resolve shorter central periods because the spectrogram looks the same for all of them, in the latter case we are not able to find the arrival time of waves of longer periods because of the constant amplitude plateau for the whole time interval. Low α deteriorates the filtration in a short period range and high α in a long period range.

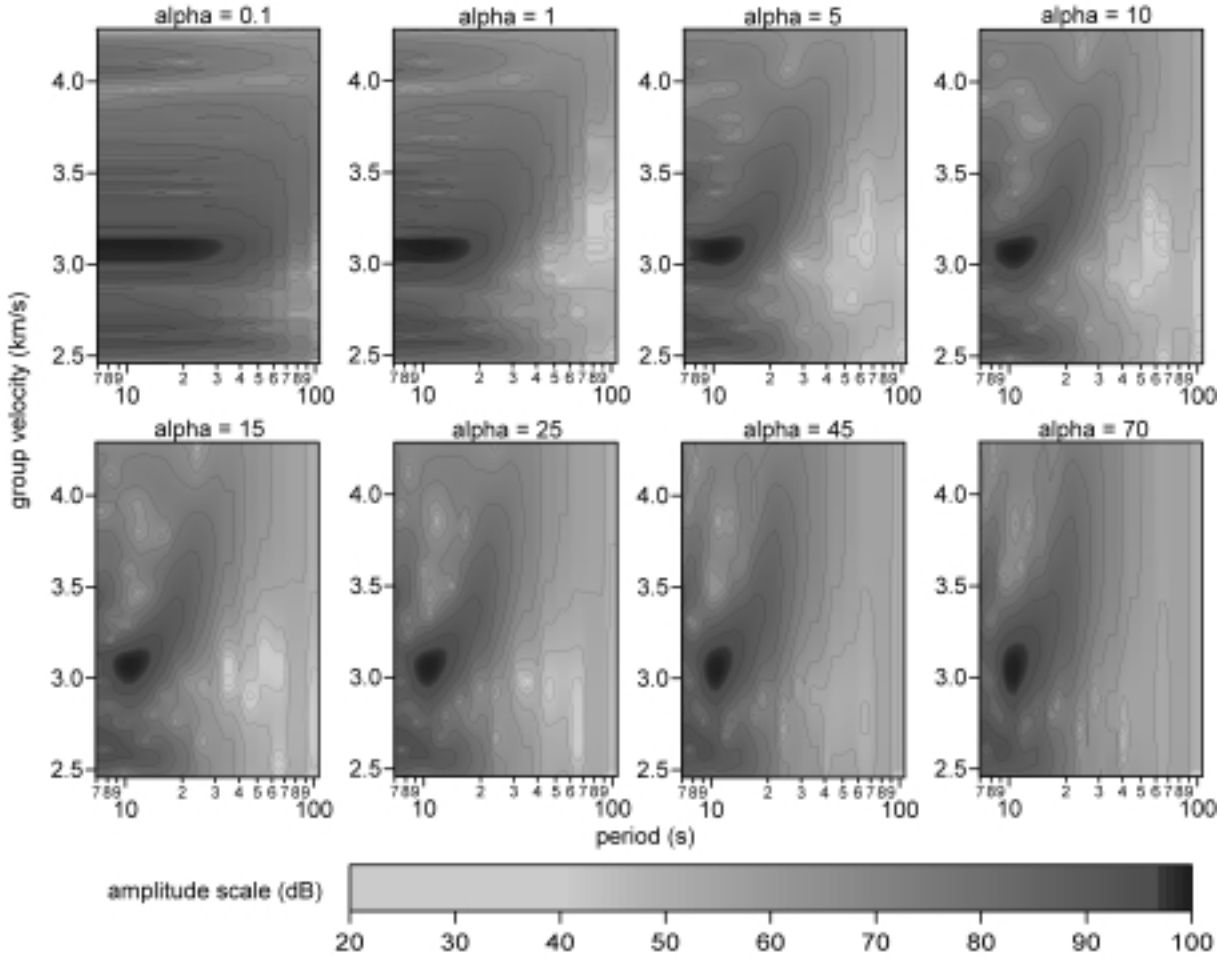

Fig. 5 Spectrograms of transverse component record of the Turkish earthquake (see Tab. 1) for eight different values of the coefficient α (alpha). All other parameters of the computing process are constant. For α = 5, the spectrogram is estimated well for long periods and for α = 45, it is estimated well for short periods. According to these spectrograms, the optimal linear dependence of coefficient α on central period T was set. The energy contours spacing is 7 dB.

The value $\alpha = 10$ keeps good energy resolution in both time and frequency domains. This value was used for homogeneous filtering to find the preliminary dispersion curves of all the processed earthquake records. The characteristics of the records was studied and the period range of fundamental modes estimated for further computing. Then, according to the process shown in Fig. 5, the linear dependence of coefficient α on the central period T was set. It is given by the expression

$$\alpha_{opt}(T) = 61.6 - 0.8 \cdot T, \tag{19}$$

where T is the original central period in seconds computed before filtering.

For T = 2.0 s α_{opt} = 60 and for T = 70.0 s α_{opt} =5.6. For $T >$ 70.0 s coefficient α was set as a constant value α_{opt} = 5. Such an optimal filtering represents smoother dispersion curves than the homogeneous filtering, but the main properties of spectrogram are visible by using the homogeneous filtering with the constant value $\alpha = 10$. The effect of constant relative resolution filtering is decreased by using the dependence given by the expression (19). The spreading of filter broadness with lower central periods is kept but it is slower than in case of a homogeneous filtering. Another expression for estimating the optimal coefficient α can be found in Levshin et al. (1972 and 1992). Equation (19) does not need the preliminary dispersion derivation $\left| dt_g(\omega)/d\omega \right|$, but the expression mentioned before does. Equation (19) is suitable for Asian earthquakes studied during this work; the expression given by Levshin et al. has general validity.

6. PREPROCESSING OF THE DATA THE PRAHA SEISMIC STATION

The seismograms processed during this work were recorded by the long-period Kirnos seismographs. The three components of a seismic velocity were recorded. The free period of the pendulum is T_s = 20.0 s. The signal is digitally sampled by 10 Hz frequency and saved on the hard disk. All the spectrograms and dispersion curves drawn into them and published in this paper are presented in raw form of original record analysis and thus their group velocity concerns the arrival time of maximum of ground motion velocity. For comparing the estimated dispersion curves with PREM-curves the arrival times of each wave were corrected according to response characteristics of the seismograph. The group velocity presented in these graphs concerns the real ground motion maximum.

EPICENTERS AND ORIGIN TIMES

The coordinates of epicenters and origin times were found in USGS/NEIC and ISC catalogues accessible on the internet.

THE EPICENTRAL DISTANCES AND AZIMUTHS

Fortran program was adjusted to compute the epicentral distances, azimuths, great circle back azimuths and time differences between the origin times and the beginnings of records. For the method of computing azimuths and lengths see Novotný and Málek (2003). The epicentral distance and the time difference is needed to estimate the absolute value of group velocity and the back azimuth was used to transform the horizontal components of the record.

TRANSFORMATION OF HORIZONTAL COMPONENTS

According to the back azimuth α the north-south (N) and the east-west (E) components were transformed using

$$\begin{pmatrix} R \\ T \end{pmatrix} = \begin{pmatrix} \cos\alpha & \sin\alpha \\ \sin\alpha & -\cos\alpha \end{pmatrix} \cdot \begin{pmatrix} N \\ E \end{pmatrix} \tag{20}$$

to the radial (R) and transverse (T) components. For positive values of the ground velocity amplitudes in the direction to the north at the N component and to the east at the E component we obtain positive values of amplitudes pointing against the propagation direction at the R component and to the right viewing in the direction of propagation at the T component, respectively. Only this geometrical transformation was used while processing the records. By minimizing of Love and Rayleigh waves amplitudes at radial versus transverse component, we can obtain better distinguishing between these two types of waves, but the absolute value of amplitude is not critical for the dispersion curves estimation.

PREM – AVERAGE DISPERSION CURVES

To compare estimated curves with average Earth model curves the PREM (Lay and Wallace, 1995) was used. Curves were computed by Fortran program built by Novotny. For matrix method used in this program see Proskuryakova et al. (1981). Only 600 km of depth from Earth surface were used.

7. EXAMPLES OF SURFACE WAVE ANALYSIS

Four examples (Fig. 8 – 11) of about forty earthquake records, processed during the work, are presented in this paper. There are also the estimated dispersion curves drawn in each spectrogram. The points obtained as a result of the SVAL program were only connected, no smoothing is applied.

Raw and filtered seismograms of all three components are shown. Red colour represents fundamental Rayleigh mode, blue is fundamental Love mode. Light red and light blue represents overtones of a corresponding wave type. Time is measured from the earthquake origin time.

In a right bottom of each figure, there is a graph comparing estimated curves (solid colour lines) with the average PREM-curves (dashed black lines). The time correction, according to the transfer function of the seismograph, is applied on these curves. Below each figure, there are parameters concerning the earthquake. Now we will discuss the analysis in details.

In Fig. 8 we see well detached groups of the fundamental Rayleigh mode at vertical and radial component and the fundamental Love mode at transverse component. Besides, there is also a strong group of fundamental Love mode at radial component. The presence of fundamental Rayleigh mode at transverse component is unclear. In Fig. 6 there is a filtered seismogram of this wavegroup, drawn for broad range of periods, and we have already discussed that this point of view is probably not correct. In Fig. 8, we can see filtered seismograph drawn only for short periods but it also does not match the fundamental Rayleigh mode at both vertical and radial component. There are only one or two peaks at the transverse component corresponding to both group velocities and a period with the remaining components. The presence of surface waves at "wrong" component could be explained by lateral heterogeneity (Levshin, 2002) due to which the waves do not propagate along the great circle path and they come to the station from another direction than the geometrical back azimuth predicts.

At the transverse component, we can see also the first higher mode (overtone) of Love waves. This phenomenon is discussed in paragraph 3. Concerning the estimation of group velocities. Overtones of

Rayleigh waves were also found. There is a coda at all three components, but only the fundamental mode of Love waves at transverse component is well separated from this coda (or from the fundamental Rayleigh mode group).

Dispersion curves of fundamental modes were estimated for period range from 7.0 and 9.0 s to 100 and 105 s for Rayleigh and Love waves respectively. The group velocities correspond to the average PREM-curves well for the period range from 8 to 15 s. By comparing the results both with PREM and the spectrograms, the Airy phase is well visible at the fundamental modes of all three components at the spectrograms.

In Fig. 9 the structure of the record is more complicated. The fundamental Rayleigh and Love modes were found at the corresponding components but also fundamental Love mode at the vertical and at the radial components is represented. The periods of main group of Love waves at radial and at vertical components exactly fit the periods of these waves at the transverse component, but the Airy phase at the "wrong" components is shifted to the lower group velocities. The first higher mode of Love waves at the transverse component and the same mode of Rayleigh waves at the vertical and at the radial component are observed. Green and pink colours represent presumed second overtones; the whole record contains many groups like that and it is not easy to interpret them.

The shape and Airy phase of the estimated fundamental modes dispersion curves correspond well with PREM-curves but the curves are shifted to a longer period range. The range of estimated periods reaches up to 100 s. The curves of the radial components are not well determined for periods over 50 s.

In Fig. 10 we can see the vertical and the radial component not as complicated as the transverse component. Both fundamental Rayleigh and Love modes were found but the Love group was weaker than the Rayleigh group. In comparison with the fundamental Love mode at transverse component, we can see that the trace of this group on the vertical and the radial components represents only the last part of the group seen at transverse component and not the strongest. It could be caused by the multipathing, when part of the wavegroup separates somewhere along its path and propagates from another direction. Such split groups come later than the main group and are recorded also at "wrong" components. There is a trace of first higher Rayleigh mode seen at both component spectrograms but the dispersion was not estimated well for these overtones due to scattered filtering of spectrogram. The filtered seismograms, belonging to these overtones, are shown only to demonstrate their presence.

The fundamental Love mode at the transverse component has a long duration and the strong first higher mode within the long periods can be also seen. The dispersion curve for the fundamental mode is drawn for broad range of periods, but over 70 s it seems to be not well estimated because the amplitudes of such waves are weak. The filtered seismogram only for periods over 9 s is shown. There is a complicated structure between the fundamental and the first higher mode seen at the spectrogram. The dispersion of the higher mode was not well estimated. Fundamental Rayleigh mode at the transverse component is estimated only for the periods shorter than the Airy phase period (about 20 – 30 s) so the filtered seismogram shows shorter periods (10 s) coming before the longer ones. No dispersion appears on the filtered seismogram, but it demonstrates well the presence of this mode at transverse component.

We can see the simple structure and well separated group of waves in Fig. 11. It is because of an oceanic path that waves propagated through. All the most important features typical for the oceanic path propagation are presented here. Short periods of Love waves (under 6 s) are absent due to the layer of water – these waves cannot propagate there. Rayleigh waves of short period (under 10 s) propagate very slowly because of the water and therefore they also cannot be seen at the part of the record which the spectrograms present. Along the oceanic path, we can see also very steep dispersion curves – the waves of nearly the same period propagate by different velocities. There is no Airy phase observed at the transverse component and only a trace of it at the vertical and the radial component.

8. DISCUSSION

Due to the filtering of nearly monochromatic signals, it is more difficult to estimate the steeper dispersion curves. It is the problem of overtones of periods from 4 to 10 s. In case of such a steep dispersion the moving-window technique could give more appropriate results. As we find a local maxima for every period (frequency) in case of multiple-filter technique, we can find such local maxima for each time (or group velocity) value in case of moving-window technique. Because of the function dependence $U(T)$, which is represented by the multiple-filter technique, the Airy phase can be well estimated. In case of time-frequency representation $T(U)$ that uses the moving window technique, the minimum of curves cannot be filtered out of the spectrogram in such a simple way because the two local maxima for given time (or group velocity) are to be looked for. There should not be this problem in case of monotonously dispersed signals.

Other methods of time-frequency analysis mentioned in literature such as moving-window autoregressive analysis or time-frequency distributions (Kacoaglu and Long, 1993) are adjusted to give higher resolution of energy distribution, which is not limited by the uncertainty principle of the Fourier transformation. There are many problems with processing the records such as the method of estimation autoregressive parameters in case of the moving-window autoregressive analysis and the presence of cross members in case of the time-frequency distribution methods. The multiple-filter technique gives better resolution than we need to estimate the dispersion. It can be seen in the inappropriate high resolution in the time scale of computed spectrograms. In our opinion, there is not a strong need to use more complicated methods of time-frequency analysis then the multiple-filter technique. The most difficult target and the main goal are not to reach high resolution of time-frequency representation but to interpret the ridges and to draw the continuous dispersion curves.

9. CONCLUSIONS

The SVAL program proved to be able to estimate the dispersion of fundamental modes of the earthquake records. The obtained points in the group velocity-period diagram can be potentially used for further inversion to estimate the average structure of the Earth crust. The procedures creating filtered spectrograms and seismograms are not necessary for the estimation of dispersion curves, but it helps to check the appropriate filtering and enables to improve the next steps to obtain the dispersion curves in a broad range of periods.

Although the used seismograph is a long-period instrument, the group velocities for periods over 60 s are not well determined because of weak amplitudes and unclear maxima of spectrogram in this period range. In a short period range, it is sometimes unclear, which of the ridges belongs to which mode. But in range from 6 to 50 s the dispersion curves are well estimated and can be used for further processing.

ACKNOWLEDGEMENTS

This work was partially supported by the grant 205/01/0481 of the Grant Agency of the Czech Republic. I would like to thank also to Vladimír Plicka and Jaromír Janský – the operators of the Praha Seismic station. The data recorded at this station were provided by the Department of Geophysics of Faculty of Mathematics and Physics of Charles University in Prague, which controls the station. The author is grateful to Oldřich Novotný for much helpful advice during the elaborating of diploma thesis, which preceded this paper, and to Jiří Málek, who carefully read the manuscript of this paper.

REFERENCES

Čermák, F.: 1990, Frequency and Time-Frequency Methods of Surface Wave Dispersion Estimation. Diploma thesis, Department of Geophysics, Faculty of Mathematics and Physics, Charles University, Prague. (Spektrální a spektrálně časové metody výpočtu disperze povrchových vln. Diplomová práce, KG MFF UK, Praha, in Czech).

Červený, V.: 2001, Seismic Ray Theory. Cambridge University Press, Cambridge, UK.

Dziewonski, A., Bloch, S. and Landisman, M.: 1969, A Technique for the Analysis of Transient Seismic Signals. Bull. Seism. Soc. Am., Vol. 59, No. 1, 427-444.

Dziewonski, A. and Anderson, D.L.: 1981, Preliminary reference Earth model. Phys. Earth Planet. Interiors, No. 25, 297 – 356.

ISC, 2001, International Seismological Centre, On-line Bulletin, http://www.isc.ac.uk/Bull, Internatl., Seis. Cent., Thatcham, United Kingdom.

Kacoaglu, A.H. and Long, L.T.: 1993, A Review of Time-frequency Analysis Techniques for Estimation of Group Velocities. Seismological Research Letters, Vol. 64, No. 2, 157 – 167.

Kolínský, P.: 2003, Dispersion of Seismic Surface Waves Along Selected Eurasian Paths. Diploma thesis, Department of Geophysics, Faculty of Mathematics and Physics, Charles University, Prague. (Disperze povrchových seismických vln podél vybraných euroasijských tras. Diplomová práce, KG MFF UK, Praha, in Czech.)

Lay, T. and Wallace, T.C.: 1995, Modern Global Seismology. Academic Press, Inc, (International Geophysics Series), San Diego.

Levshin, A., Pisarenko, V.F. and Pogrebinsky, G.A.: 1972, On a Frequency-Time Analysis of Oscillations. Ann. Geophys., Vol. 28, No. 2, 211-218.

Levshin, A.L., Ratnikova, L. and Berger, J.: 1992, Pecularities of Surface-Wave Propagation Across Central Aurasia. Bull. Seism. Soc. Am., Vol. 82, No. 6, 2464-2493.

Levshin, A.L.: 2002, Surface Wave Analysis and Phenomenology, 6th Workshop on Three-Dimensional Modeling of Seismic Waves Generation and their Propagation. The Abdus Salam International Centre for Theoretical Physics, September – October 2002.

Novotný, O. and Málek, J.: 2003, Note on the Direct Computation of Geodetic Distances and Azimuths on an Ellipsoid of Revolution. Acta Montana, IRSM AS CR, ser. A, No. 22 (129), 75-78.

Press, H.W., Teukolsky, S. A., Vetterling, W. T. and Flannery, B.P.: 1992, Numerical Recipes in Fortran, (World Wide Web Sample). Cambridge University Press, Cambridge, UK.

Proskuryakova, T.A., Novotny, O. and Voronina, E.V.: 1981, Studies of the Earth's Structure by the Surface-Wave Method (Central Europe). Nauka, Moscow, (Izuchenie stroeniya Zemli metodom poverkhnostnykh voln (Tsentral'naya Evropa). Nauka, Moskva, in Russian).

Sekereš, J.: 1983, Frequency-time analysis. Diploma thesis, Department of Geophysics, Faculty of Mathematics and Physics, Charles University, Prague. (Frekvenčne-časová analýza. Diplomová práce, KG MFF UK, Praha, in Slovak.)

USGS/NEIC, 2003, United States Geological Survey / National Earthquake Information Centre (Earthquake Hazards Program), http://neic.usgs.gov/neis/bulletin.

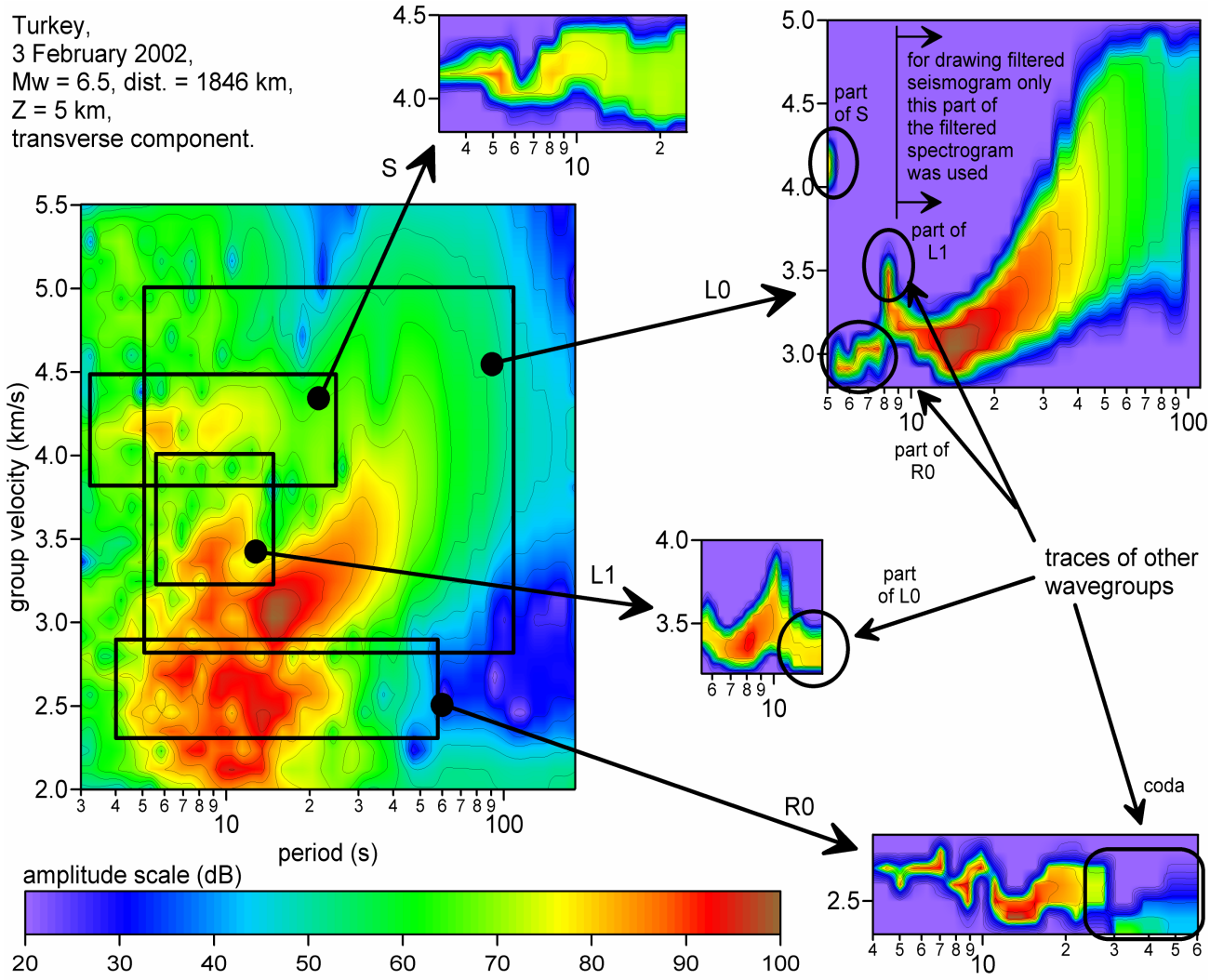

Fig. 6 Spectrogram of the transverse component of the Turkish earthquake record (see Tab. 1) is shown. The four rectangles represent a selection of three dispersive surface wave modes (L_0, L_1 and R_0) and one non-dispersive ridge of body S wave. Examples of wrong filtering at spectrograms of surface wave modes are visible. Compare the selected and filtered spectrograms with filtered seismograms presented in Fig. 7. The colour amplitude scale has been also used for imaging figures on the next two pages. The energy contours spacing is 5 dB.

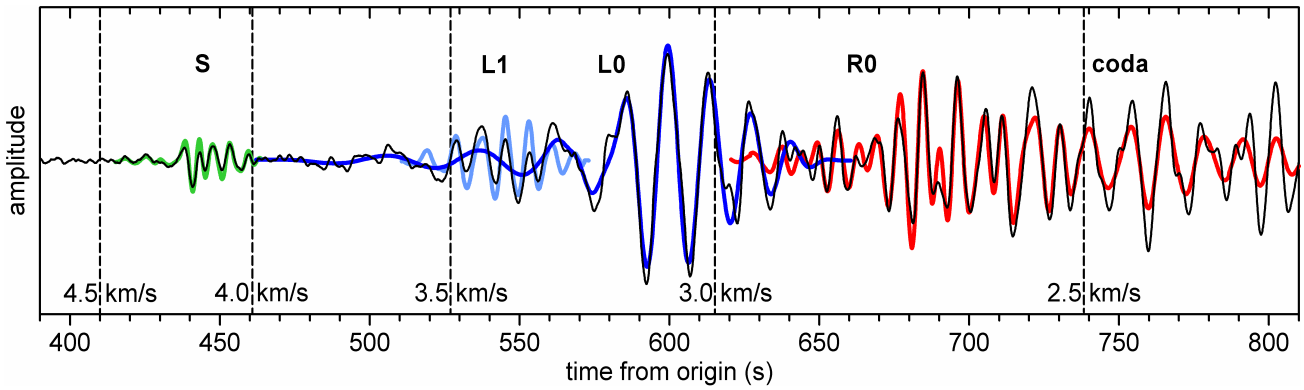

Fig. 7 Four selected ridges presented in Fig. 6 were used to create the corresponding filtered seismograms. Three dispersed surface wave modes (L_0 – blue line, L_1 – light blue line, R_0 – red line) and also body S wave (green line) are shown. The first higher mode of Love wave L_1 is clearly visible within the long periods of Love fundamental mode L_0. The original seismogram is drawn by thin solid black line. Five points of group velocity are marked.

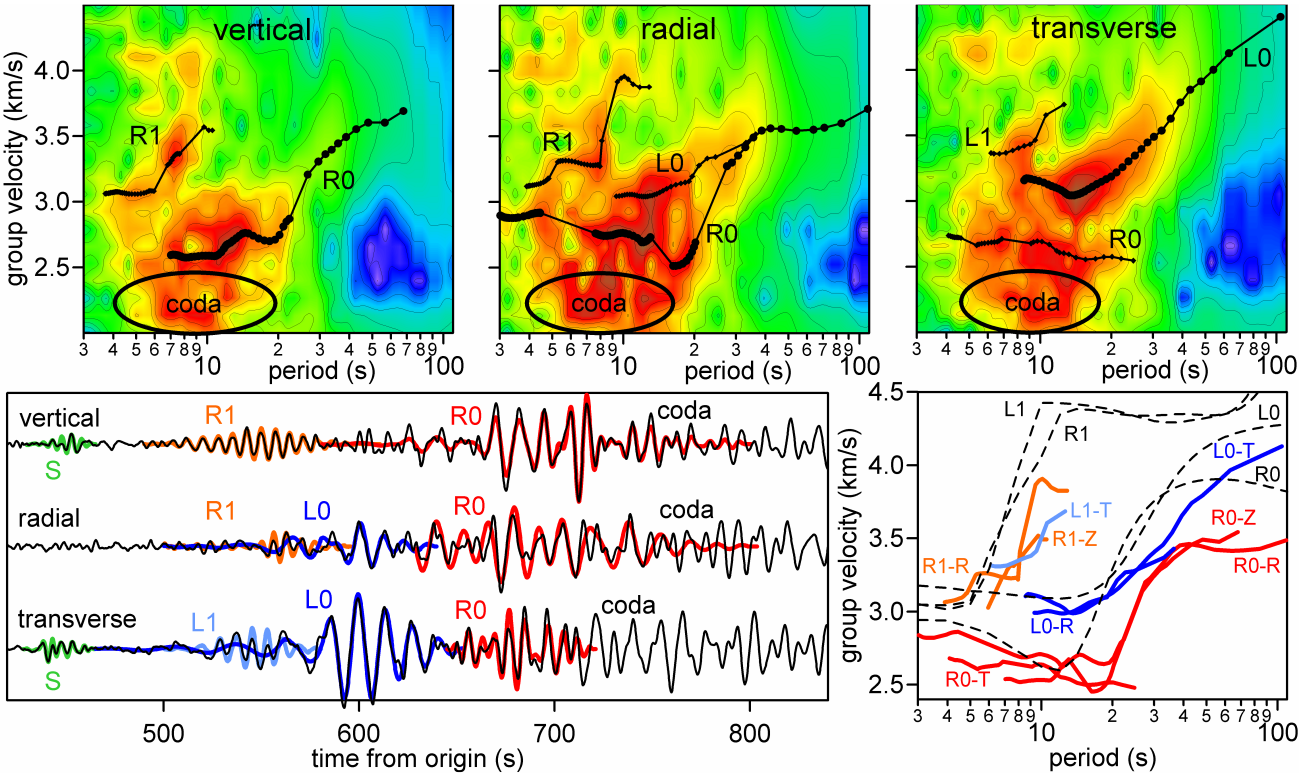

Fig. 8 Surface wave analysis of three-component record of the earthquake in Turkey; 3 February 2002; epicenter coordinates 38.57 N, 31.27 E; epicentral distance to the Praha seismic station Δ = 1846 km; magnitude M_W = 6.5; depth Z = 5 km. The same colour amplitude scale as in Fig. 6 is used for imaging all of the spectrograms. The energy contours spacing is 5 dB.

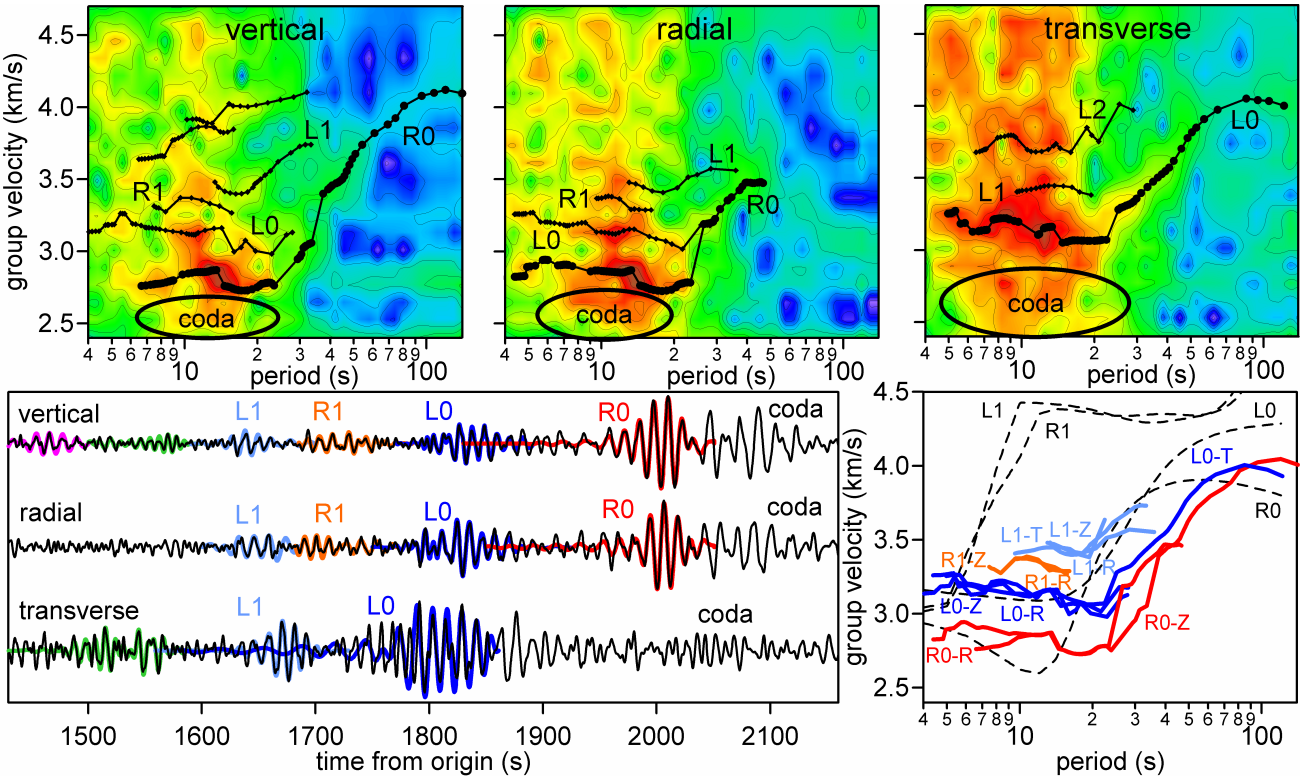

Fig. 9 Surface wave analysis of three-component record of the earthquake in Tibet; 28 March 1999; epicenter coordinates 30.51 N, 79.40 E; epicentral distance to the Praha seismic station Δ = 5731 km; magnitude M_S = 6.6; depth Z = 15 km. The energy contours spacing is 5 dB.

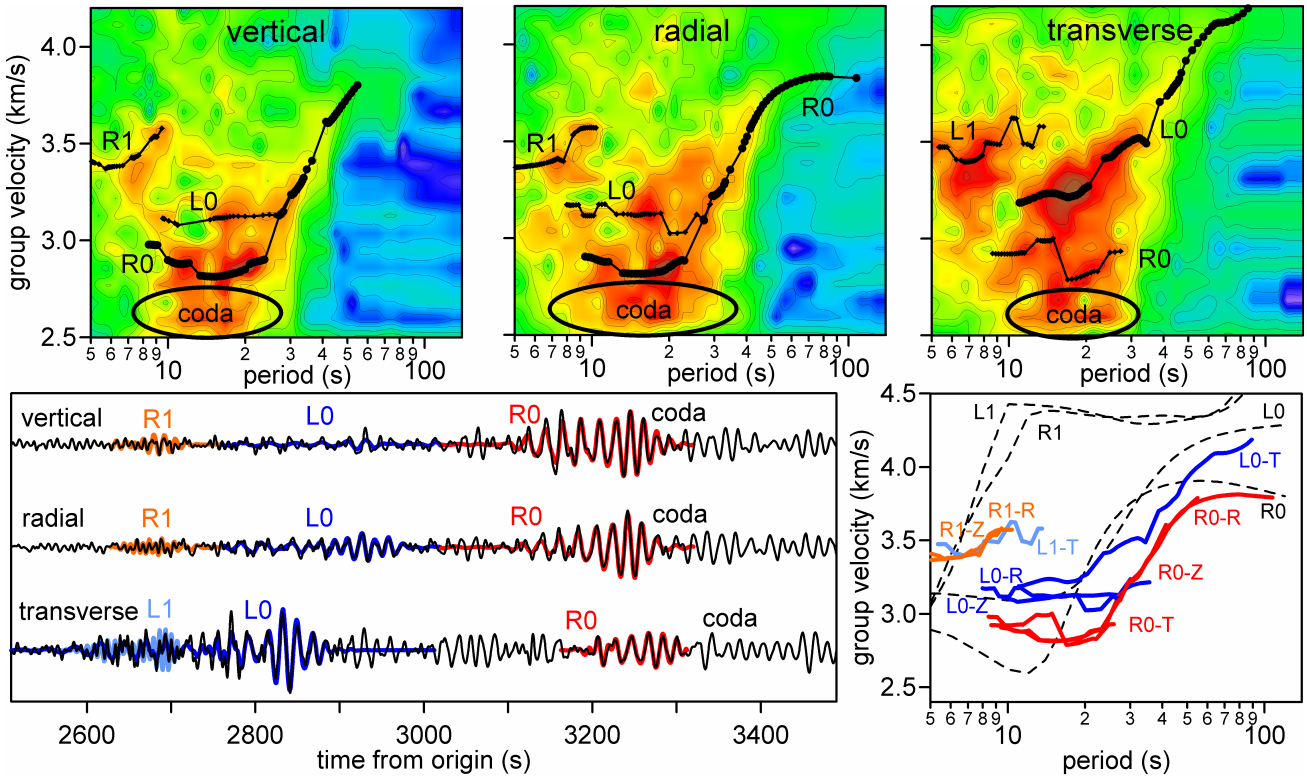

Fig. 10 Surface wave analysis of three-component record of the earthquake in Taiwan; 31 March 2002; epicenter coordinates 24.28 N, 122.18 E; epicentral distance to the Praha seismic station Δ = 9149 km; magnitude M_S = 7.4; depth Z = 32 km. The energy contours spacing is 3 dB.

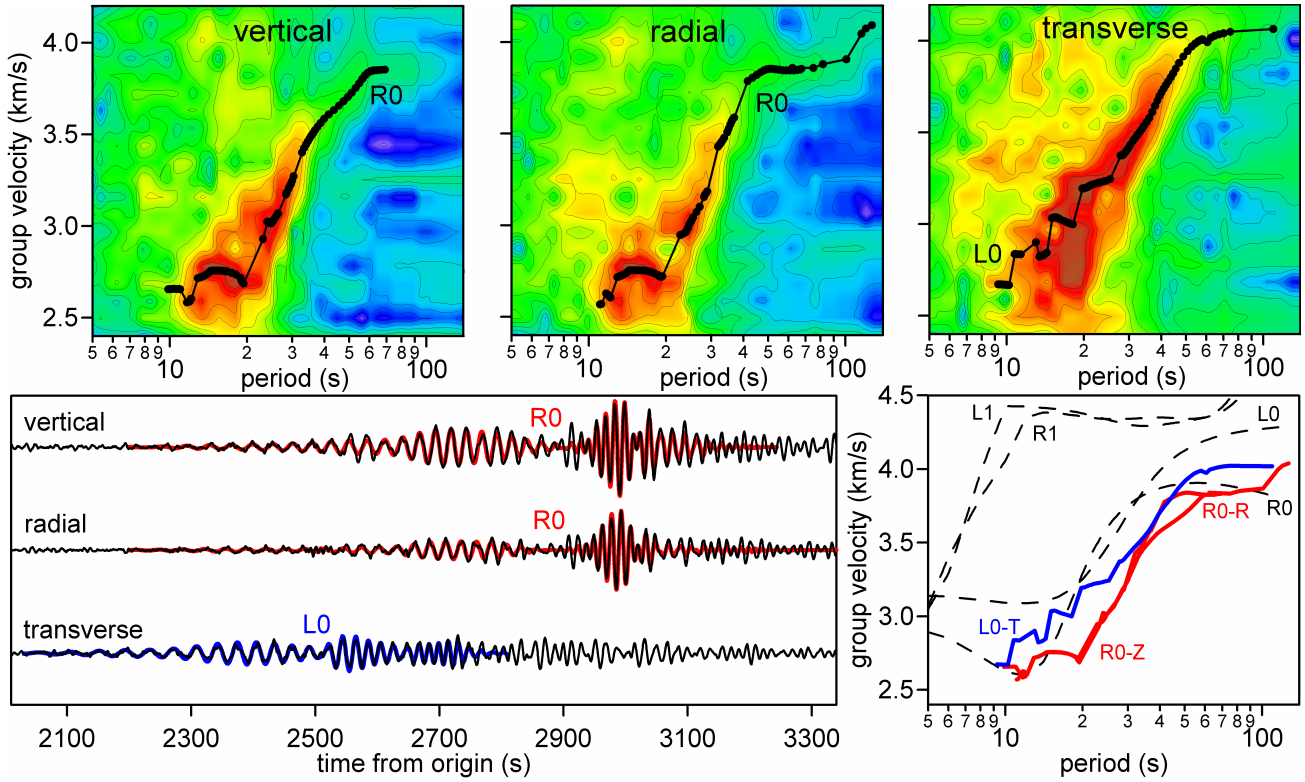

Fig. 11 Surface wave analysis of three-component record of the earthquake in Kamtchatka; 8 March 1999; epicenter coordinates 52.06 N, 159.52 E; epicentral distance to the Praha seismic station Δ = 8217 km; magnitude M_W = 7.0; depth Z = 56 km. The energy contours spacing is 3 dB.